



**HAL**  
open science

## Direct measurement of near-nano-Newton forces developed by self-organizing actomyosin fibers bound $\alpha$ -catenin

Surabhi Sonam, Clémence Vigouroux, Antoine Jégou, Guillaume Romet - Lemonne, Christophe Le Clainche, Benoit Ladoux, René Marc Mège

### ► To cite this version:

Surabhi Sonam, Clémence Vigouroux, Antoine Jégou, Guillaume Romet - Lemonne, Christophe Le Clainche, et al.. Direct measurement of near-nano-Newton forces developed by self-organizing actomyosin fibers bound  $\alpha$ -catenin. *Biology of the Cell*, 2021, 10.1111/boc.202100014 . hal-03368358

**HAL Id: hal-03368358**

**<https://hal.science/hal-03368358>**






Submitted on 7 Oct 2021

**HAL** is a multi-disciplinary open access archive for the deposit and dissemination of scientific research documents, whether they are published or not. The documents may come from teaching and research institutions in France or abroad, or from public or private research centers.

L'archive ouverte pluridisciplinaire **HAL**, est destinée au dépôt et à la diffusion de documents scientifiques de niveau recherche, publiés ou non, émanant des établissements d'enseignement et de recherche français ou étrangers, des laboratoires publics ou privés.

## RESEARCH ARTICLE

# Direct measurement of near-nano-Newton forces developed by self-organizing actomyosin fibers bound $\alpha$ -catenin

Surabhi Sonam<sup>1</sup> | Clémence Vigouroux<sup>2</sup> | Antoine Jégou<sup>1</sup>  |  
Guillaume Romet-Lemonne<sup>1</sup>  | Christophe Le Clainche<sup>2</sup>  | Benoit Ladoux<sup>1</sup>  |  
René Marc Mège<sup>1</sup> 

<sup>1</sup> Université de Paris, CNRS, Institut Jacques Monod, Paris, France

<sup>2</sup> Institute for Integrative Biology of the Cell (I2BC), Université Paris-Saclay, CEA, CNRS, Gif-sur-Yvette, France

**Correspondence**

Benoit Ladoux and René Marc Mège, Université de Paris, CNRS, Institut Jacques Monod, Paris, France.

Email: benoit.ladoux@ijm.fr;  
rene-marc.mege@ijm.fr

**Current address**

Surabhi Sonam, D Y Patil International University, Pune, India.

**Funding information**

the European Research Council, Grant/Award Number: CoG-617233; ARC Foundation, Grant/Award Number: PJA.20151203185; LABEX Who Am I?, Grant/Award Number: ANR-11-LABX-0071; La Ligue Contre le Cancer: Equipe labellisée 2019; Agence Nationale de la Recherche, Grant/Award Number: ANR-17-CE13-0013

**Background Information:** Actin cytoskeleton contractility plays a critical role in morphogenetic processes by generating forces that are then transmitted to cell–cell and cell-ECM adhesion complexes. In turn, mechanical properties of the environment are sensed and transmitted to the cytoskeleton at cell adhesion sites, influencing cellular processes such as cell migration, differentiation and survival. Anchoring of the actomyosin cytoskeleton to adhesion sites is mediated by adaptor proteins such as talin or  $\alpha$ -catenin that link F-actin to transmembrane cell adhesion receptors, thereby allowing mechanical coupling between the intracellular and extracellular compartments. Thus, a key issue is to be able to measure the forces generated by actomyosin and transmitted to the adhesion complexes. Approaches developed in cells and those probing single molecule mechanical properties of  $\alpha$ -catenin molecules allowed to identify  $\alpha$ -catenin, an F-actin binding protein which binds to the cadherin complexes as a major player in cadherin-based mechanotransduction. However, it is still very difficult to bridge intercellular forces measured at cellular levels and those measured at the single-molecule level.

**Results:** Here, we applied an intermediate approach allowing reconstruction of the actomyosin- $\alpha$ -catenin complex in acellular conditions to probe directly the transmitted forces. For this, we combined micropatterning of purified  $\alpha$ -catenin and spontaneous actomyosin network assembly in the presence of G-actin and Myosin II with microforce sensor arrays used so far to measure cell-generated forces.

**Conclusions:** Using this method, we show that self-organizing actomyosin bundles bound to micrometric  $\alpha$ -catenin patches can apply near-nano-Newton forces.

**Significance:** Our results pave the way for future studies on molecular/cellular mechanotransduction and mechanosensing.

**KEYWORDS**

$\alpha$ -catenin, actomyosin, cell–cell adhesion, mechanical force, micro force sensing arrays

## INTRODUCTION

Tissues are formed by cells adhering to the extracellular matrix (ECM). Adherent cells are interconnected by intercellular junctions that maintain their cohesion and

restrain their individual migration. Under certain physiological (embryonic development, renewal of normal tissue, wound repair) and pathological conditions (tumor transformation and invasion), cells need to extensively reshape their cell–ECM and cell–cell contacts to allow

them to migrate on the ECM and exchange their neighbors. Actin cytoskeleton contractility plays a critical role in these morphogenetic processes by generating forces that are then transmitted to cell-ECM and cell-cell adhesion complexes (Blanchoin et al., 2014). This not only allow cells to apply traction forces on the ECM and their surroundings, but also to organize, reshape and strengthen cell-ECM and cell-cell adhesions (Mege & Ishiyama, 2017; Wolfenson et al., 2019). In return, the mechanical load imposed by the environment, sensed at cell adhesion sites and transmitted to the cytoskeleton, influences cellular processes such as cell migration, differentiation and survival (Discher et al., 2005). In this context, a key issue is to understand the mechanical coupling of cell-ECM and cell-cell adhesions and the actomyosin network. One of the first steps toward this objective is to be able to measure the forces applied by actomyosin on adhesion complexes.

Cells generate and respond to mechanical force through changes in internal tension imposed by non-muscle myosin II (Myosin II) on the F-actin network (Blanchoin et al., 2014; Vicente-Manzanares et al., 2009). Anchoring of the actomyosin cytoskeleton to adhesion sites is mediated by adaptor proteins that link F-actin to transmembrane cell adhesion receptors, thereby allowing mechanical coupling between the intracellular and extracellular compartments. This coupling is best known for cell-ECM adhesions mediated by integrins and cell-cell adhesions mediated by cadherins. It involves the transduction of the mechanical cues into intracellular biochemical reactions that cause actomyosin cytoskeleton re-organization and adhesion complexes assembly, thereby directing tension-dependent growth of these adhesions (Mege & Ishiyama, 2017; Wolfenson et al., 2019). The whole process allows cells to sense, signal, and respond to changes in both cell's internal contractility and in environment mechanical properties. It is therefore a very dynamic and complex process, integrating cellular, subcellular and molecular scale responses. It remains, however, very difficult to integrate in the general picture forces measured on the one hand at the molecular level (del Rio et al., 2009; Grashoff et al., 2010; Yao et al., 2014) and on the other hand at the cellular level (Ladoux et al., 2010; Sarangi et al., 2017).

The forces transmitted at cadherin-mediated cell-cell contacts have been first measured at the cellular level thanks to recombinant cadherin coated  $\mu$ FSA (micro-Force Sensor Arrays) (Ganz et al., 2006). They are in the range of tens of nanoNewtons (nN), close to the magnitude of forces transmitted by integrin at cell-ECM contacts. Further analysis allowed to demonstrate that these adhesions are also mechanosensitive (Ladoux et al., 2010). Approaches developed in cells, and those probing the mechanical properties of single  $\alpha$ -catenin molecules, allowed to identify  $\alpha$ -catenin, an F-actin binding protein which binds to the cadherin cytoplasmic

tail via  $\beta$ -catenin as a major player in cadherin-based mechanotransduction and mechanosensing (Buckley et al., 2014; le Duc et al., 2010; Mege & Ishiyama, 2017; Seddiki et al., ; Thomas et al., 2013; Yao et al., 2014; Yonemura et al., 2010). However, considering the mere transmission of forces at cell-cell contact, it is still very difficult to bridge intercellular forces measured at cellular levels (in the tens of nN range) and those measured at the single molecule level ( $\approx 5$  pN) as measured by FRET-based  $\alpha$ -catenin molecular sensors (Grashoff et al., 2010; Kim et al., 2015). An alternative intermediate approach based on reconstituted molecular networks comprising dynamic actomyosin assembly in vitro was developed to quantify the force-dependent association of protein complexes involved in cell-ECM mechanotransduction (Ciobanasu et al., 2014; Ciobanasu et al., 2015), but lacked force measurement.

Here, we applied this intermediate approach to reconstitute the mechanical link between  $\alpha$ -catenin and actomyosin with pure proteins and probe the transmitted forces. We used micropatterning of purified  $\alpha$ -catenin and spontaneous actomyosin network assembly in the presence of G-actin, Myosin II and ATP, as developed previously to reconstruct the talin actomyosin link (Ciobanasu et al., 2015). We combined this approach with PDMS (polydimethylsiloxane) micropillars sensor arrays ( $\mu$ FSA), extensively used so far to measure cell generated forces (Trichet et al., 2012; Vedula et al., 2012), to measure forces developed by  $\alpha$ -catenin-bound actomyosin bundles.

## RESULTS

$\alpha$ -catenin-coated  $\mu$ FSAs (3  $\mu$ m in diameter and 12  $\mu$ m in height), arranged as doublets, with 20  $\mu$ m inter-pillar and 100  $\mu$ m inter-doublet distances were prepared as described in "Methods and Materials" (Figure 1a). To ensure the attachment of the protein on the top of the pillars, we adapted a previously developed micropatterning protocol (Melerio et al., 2019; Pasturel et al., 2019). Briefly,  $\mu$ FSAs were first coated with poly-L-lysine (PLL) and poly (ethylene glycol) succinimidyl valerate (PEG-SVA) to create a non-adhesive layer. Passivated  $\mu$ FSAs were then placed on an inverted microscope and illuminated with ultraviolet light (375 nm) passing through a digital photomask in the presence of photo initiator. The photomask was generated from the imaging of the arrays of micropillar doublets themselves, which allowed burning the PLL-PEG-SVA layer exactly on the top surface of micropillars (Pasturel et al., 2019).  $\mu$ FSAs were then rinsed, incubated with purified  $\alpha$ -catenin, blocked with BSA, and washed again with a coating buffer.  $\alpha$ -catenin-coated  $\mu$ FSAs were then placed on a glass coverslip with spacers on the side. Protein-coated  $\mu$ FSAs were eventually submerged within freshly prepared actin polymerization mix containing KCl, ATP,

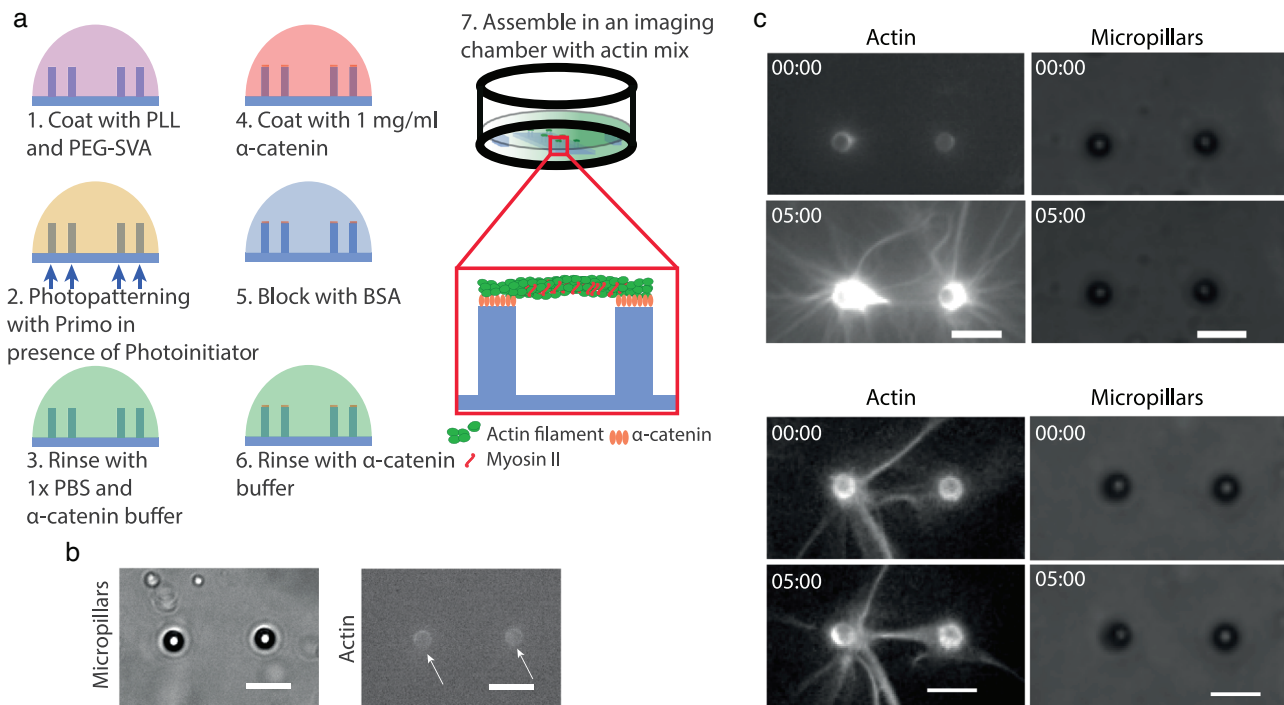


**FIGURE 1** Reconstitution of the actomyosin/ $\alpha$ -catenin link in acellular conditions. (a) Schematic showing the protocol followed for the coating of  $\alpha$ -catenin and attachment of actin filaments on micropillars. (b) Representative image of a doublet of micropillars (bright field; above) and white arrows showing fluorescent polymerized actin attached to them (actin mix containing  $2.4 \mu\text{M}$  G-actin). (c) Representative images of actin filaments on micropillars at time 0 (00:00) and after 5 min of imaging (05:00). An actin bundle forms and thickens between the two micropillars. Data were recorded for  $1.2 \mu\text{M}$  G-actin and  $100 \text{ nM}$  myosin II concentrations (upper panel), and for  $2.4 \mu\text{M}$  actin and  $100 \text{ nM}$  myosin II concentration (lower panel). Scale bars =  $10 \mu\text{m}$

unlabeled G-actin and fluorescently labelled G-actin (98:2 ratio), covered with a coverslip to prevent evaporation and then directly placed under microscope for imaging (Figure 1a). After a few minutes, fluorescent F-actin was detected on the  $\alpha$ -catenin-coated micropillars (Figure 1b). When the experiment was repeated on  $\mu\text{FSAs}$  coated with BSA only, no fluorescent actin was detected at the micropillar tips indicating that recruited F-actin was specifically bound to  $\alpha$ -catenin.

We then analyzed the evolution of the polymerizing actin network in the presence of myosin II mini-filaments ( $100 \text{ nM}$ ). The experiments were performed for two initial concentrations of G-actin ( $1.2$  and  $2.4 \mu\text{M}$ ) (Figure 1c). At both G-actin concentrations, thick F-actin bundles grow in solution, some anchored to the micropillar tips. Some of them specifically developed between the twin  $\alpha$ -catenin-coated micropillars (Figure 1c). Inter-pillar F-actin bundles connecting  $\alpha$ -catenin-coated pillars were not detected in the absence of myosin II.

In line with cell force measurements on  $\mu\text{FSAs}$  (Trichet et al., 2012), following micropillar tip positions in bright field over time allowed us to evaluate whether pillars are deflected due to forces generated by actomyosin cables bound to them. Small displacements of twin pillar tips were observed, indicating that contractile forces applied by actomyosin bundles to  $\alpha$ -catenin-coated micropillars

are sufficient to induce their deflection. We further quantified the pillar tip displacements over time in the presence of  $2.4 \mu\text{M}$  of G-actin and  $100 \text{ nM}$  of myosin II (Figure 2a). Plotting the displacement of micropillar tips over time revealed that individual micropillars of the twin gradually bended inward towards each other as actomyosin network built up over time, before plateauing (Figure 2a). In the absence of either myosin II or  $\alpha$ -catenin, there was no significant change in inter-pillar distances (Figure 2c), indicating that the deflections require the binding of an active actomyosin network on micropillars. To ensure that the observed pillar deflections were indeed due to the contraction of the inter-pillar actomyosin bundles, we plotted the deflection of one micropillar as a function of the deflection of the other micropillar of the pair (Figure 2b). Deflection of the twin micropillars were highly correlated (Spearman correlation,  $r = 0.9668$ ), indicating that equal forces were applied on each pillar as expected for forces generated by inter-pillar actomyosin bundles. Thus, in this configuration, forces applied on the micropillars by the meshwork of actomyosin in the bulk are negligible and/or cancel each other.

This saturation in the curves pillar displacement versus time could reflect the progressive mobilization of inter-pillar contractile actomyosin bundles up to maximum for given G-actin and myosin II concentrations.

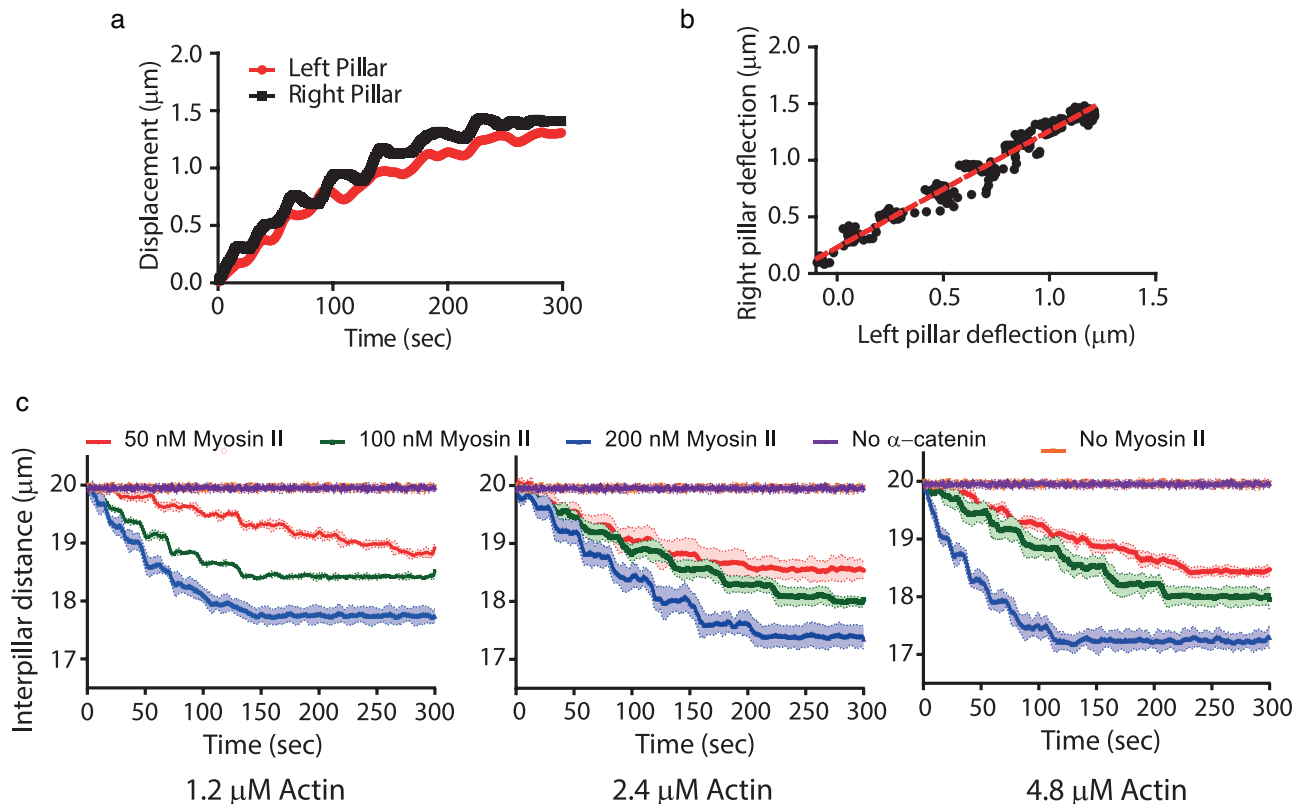


**FIGURE 2** Micropillar deflections under actomyosin tension. (a) Graphs showing displacement over time of each single micropillar within a pair in the presence of G-actin  $2.4 \mu\text{M}$  and myosin II  $100 \text{ nM}$ . Both left pillar (red) and right pillar (black) gradually bend toward each other over time. (b) Plot of left and right displacement magnitude plotted against each other. Deflections of left and right pillars are correlated in time. Black dots represent the values of left and right pillar deflections and red dotted line is the straight line fit to the scatter plot. (Spearman correlation,  $r = 0.9668$ ). (c) Plots of inter-pillar distance as a function of time for three sets of G-actin concentrations ( $1.2$ ,  $2.4$ , and  $4.8 \mu\text{M}$ ) in the presence of  $50$ ,  $100$  and  $200 \text{ nM}$  Myosin II, or in the absence of Myosin II or of  $\alpha$ -catenin. Pillar deflections were measured every second for  $5 \text{ min}$ . Each curve represents the mean ( $\pm\text{SEM}$ ) of  $5$  to  $6$  data sets obtained from three independent experiments. Inter-pillar distance decreases with time for all conditions except when no  $\alpha$ -catenin was coated on micropillars or when no myosin was added

Thus, we then plotted the evolution of the inter-pillar distance over time for a combination of different concentrations of G-actin ( $1.2$ ,  $2.4$ , and  $4.8 \mu\text{M}$ ) and myosin II ( $50$ ,  $100$ , and  $200 \text{ nM}$ ) (Figure 2c). For all concentrations, we confirmed a saturable decay in the inter-pillar distance as a function of time. In addition, for a given concentration of myosin, we observed a decrease in the minimum inter-pillar distance reached at the plateau when increasing actin concentrations. For example, in presence of  $50 \text{ nM}$  myosin, increasing actin concentration from  $1.2$  to  $2.4 \mu\text{M}$  and  $4.8 \mu\text{M}$  led to a decrease in the equilibrium inter-pillar distance from  $19.02 \pm 0.05$  to  $18.43 \pm 0.15 \mu\text{m}$  and to  $17.76 \pm 0.14 \mu\text{m}$ . Similarly, for a fixed G-actin concentration, the minimum inter-pillar distance reduced with the increase in myosin concentration (for example from  $19.02 \pm 0.05 \mu\text{m}$  to  $18.55 \pm 0.19 \mu\text{m}$  to  $18.43 \pm 0.07 \mu\text{m}$  for  $50$ ,  $100$  and  $200 \text{ nM}$  myosin, respectively). Thus, these observations indicate that micropillar twins are deflected inward by actomyosin bundles linking them up to a saturation point set by the amount of actomyosin that can be mobilized at equilibrium.

Micropillar deflection has been extensively used to extract the forces applied by single cell (du Roure et al., 2005; Saez et al., 2010; Tan et al., 2003; Vedula et al., 2012) based on the equation of linear theory of elasticity, that is, the force applied on each pillar is obtained by multiplying its deflection by its spring constant calculated from pillar dimensions and elastic modulus of PDMS (see “Methods and Materials”). With this, we could plot the instantaneous force applied per micropillar as a function of time for various concentrations of G-actin ( $1.2$ ,  $2.4$ , and  $4.8 \mu\text{M}$ ) and myosin II ( $50$ ,  $100$ , and  $200 \text{ nM}$ ) (Figure 3). As expected from the observed evolution over time of inter-pillar distances, the force applied on micropillars increased with an initial linear phase to then saturate after a few minutes (Figure 3a-c). However, both the rate of force increase and the force at the plateau increased with both G-actin and myosin II concentrations. For example, increasing myosin II concentrations from  $50$  to  $100 \text{ nM}$  and  $200 \text{ nM}$  for a given concentration of G-actin ( $1.2 \mu\text{M}$ ) increased almost linearly the force magnitude at which the force evolution saturates, from

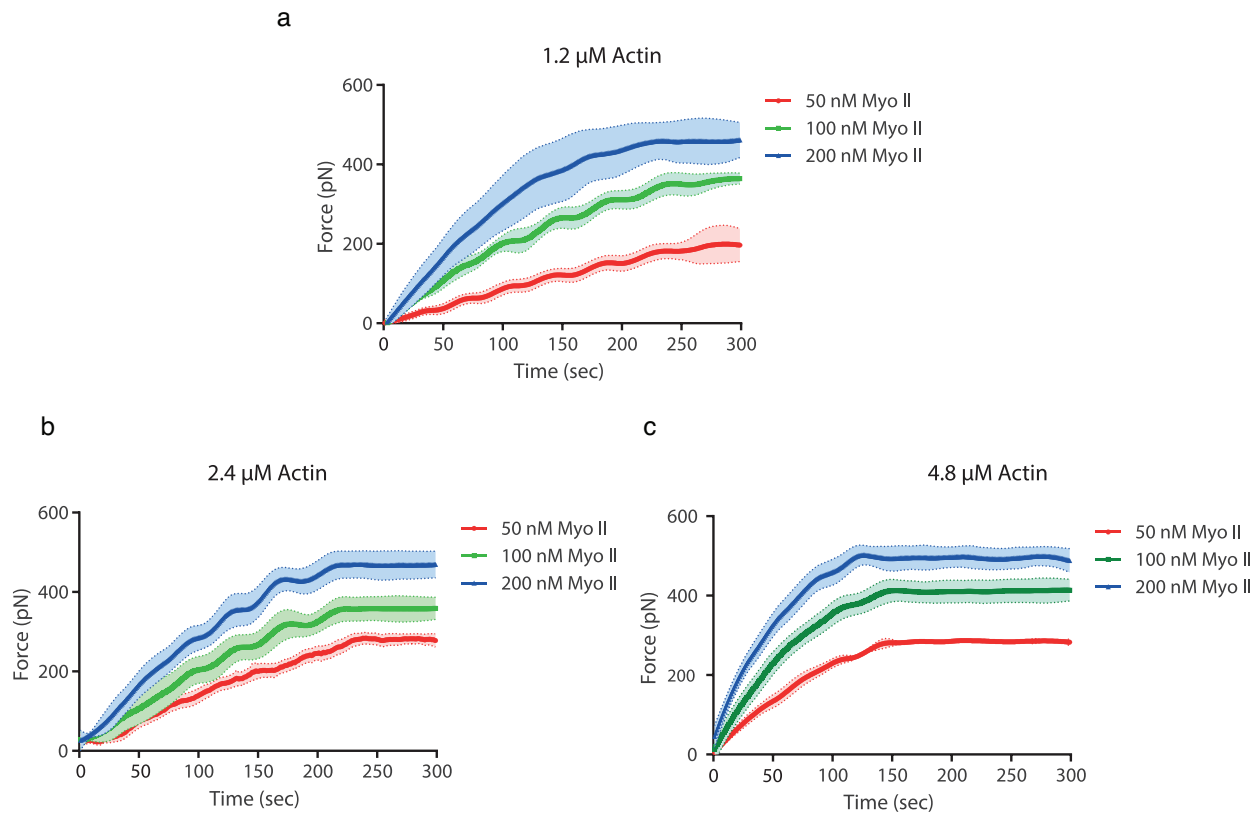


**FIGURE 3** Evolution over time of the forces applied per pillar. Mean force ( $\pm$ SEM) over time were plotted for three myosin II concentrations (50, 100, and 200 nM) at three fixed G-actin concentrations: 1.2  $\mu\text{M}$  (a), 2.4  $\mu\text{M}$  (b) and 4.8  $\mu\text{M}$  (c). In all conditions, the force increases with time and plateaus after a few minutes. Five to eight individual sets of pillar deflections were quantified for each curve, within three independent experiments. Pillar deflections were measured every second for 5 min

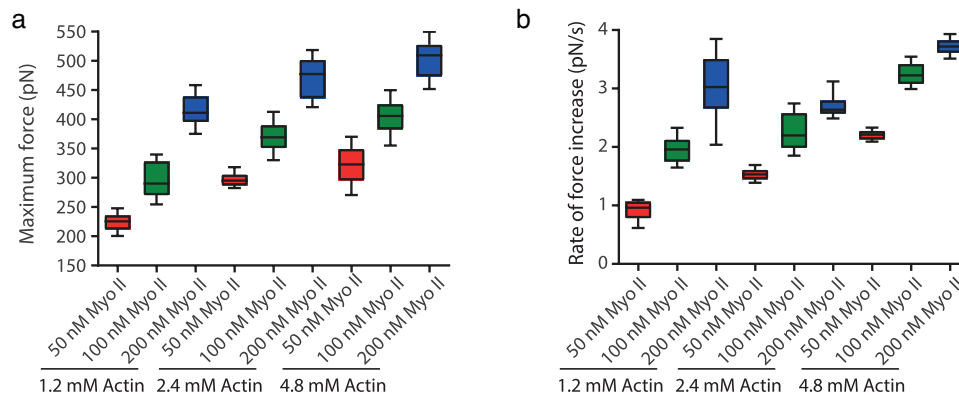


**FIGURE 4** Maximum force and initial rate of force increase. Maximum force at the plateau (a) and initial rate of force increase (b) for the different conditions of actin and myosin II concentrations. Thirty sets of data from three independent experiments were used for these box plots

223.9  $\pm$  14.6 pN, to 297.2  $\pm$  28.4 pN and 413.7  $\pm$  25.8 pN, respectively. The same linear evolution of the force magnitude at the plateau as a function of increasing myosin II concentration was observed for the two other concentrations of G-actin. Similarly, for a fixed concentration of myosin II (50 nM), the maximum force reached at the plateau increased from 223.9  $\pm$  14.6 pN, 297.2  $\pm$  10.7 pN and 321  $\pm$  30.1 pN for G-actin concentrations of 1.2, 2.4, and 4.8  $\mu\text{M}$ , respectively. The maximum force magnitude also increased with G-actin concentration

at the other two myosin II concentrations (Figure 4a). The rate of initial force evolution over time for a given G-actin concentration (1.2  $\mu\text{M}$ ) also increased with myosin II concentration from 0.9  $\pm$  0.2, 1.9  $\pm$  0.2 to 3.0  $\pm$  0.5 pN/s, respectively. The rate of force increase with time was also proportional to Myosin II concentration at the two other fixed G-actin concentrations (Figure 4b). Similarly, for given a Myosin II concentrations, the initial rate of force increase over time increased with G-actin concentration. Thus, altogether these results show that

these self-organized actomyosin bundles can apply near-nano-Newton forces.

## DISCUSSION

Taken together, we developed a platform based on  $\mu$ FSA which measures force generated by multi-protein interactions, allowing for the first time to directly quantify the force build-up by auto-assembled actomyosin cables. So far, studies have used  $\mu$ FSA to studying forces developed by single cells or multi-cellular assemblies (Desai et al., 2009; du Roure et al., 2005; Saez et al., 2010; Tan et al., 2003; Trichet et al., 2012; Vedula et al., 2012). Here, we successfully used  $\mu$ FSA to evaluate a subcellular process by reconstituting a multi-protein interaction. First, we allowed actomyosin bundles to assemble and grow on the  $\alpha$ -catenin patterns atop micropillars. Once the actomyosin bundles from each micropillar of the doublet interacted, they formed cables as expected from previously reconstituted acto-myosin networks on 2D patterned surfaces (Ciobanasu et al., 2014; Reymann et al., 2012). But, compared to these previous reports, the implementation of this approach on  $\mu$ FSA allowed to measure forces applied on the coated patterns. Attempts to grow actomyosin (Maier & Haraszti, 2015; Roos et al., 2003) and microtubule (Roos et al., 2005) networks on micropillars have been reported previously but were not intended, and did not achieve the conditions required to measure forces applied by the network. Indeed, in these assays, the networks form in between micropillars and their growth could not be restricted to the top of the  $\mu$ FSA, a prerequisite to infer the applied forces from the deflection of the pillars. Here thanks to the use of local DMD-assisted PEG burning specifically on the pillar tips (Pasturel et al., 2019), we were able to restrict actin filament binding to the top of the pillars. Spatz and coworkers published another approach where a few actin filaments held by beads trapped by optical tweezers allowing to measure pulling forces in the range of fractions of pN (Streichfuss et al., 2011). This is, however, way below the force developed by single Myosin II motors (Finer et al., 1994), or needed to unfold a single  $\alpha$ -catenin molecules (Yao et al., 2014) which have been reported to be in the range of a few pN. In the present study, the measure forces varied from 200 to 500 pN, depending upon the actin monomer and myosin II concentrations; thus, likely associated to multiple actin filaments and myosin motors. As expected both the maximum force at equilibrium and the rate at which force increased were proportional to G-actin and myosin concentrations, although at the present stage we cannot evaluate the number of actin filaments in the bundles nor the number of  $\alpha$ -catenin bound to them. We believe that our system is of sufficient sensitivity and accuracy to further address the molecular mechanisms associated with cadherin-catenin mechanotransduction

and mechanosensing. Indeed, experiments performed in the absence of  $\alpha$ -catenin or of myosin II serving as negative controls, where pillar position fluctuations are due to thermal noise and/or other fluctuations in the system, provide a baseline to evaluate how precisely we can measure micropillar position. Pillar position fluctuating below 0.1  $\mu$ m in these conditions allowed us to estimate the accuracy of the force measurement in the range of 3.5 pN.

In conclusion, by allowing measurements of force generated by multiple actomyosin cables on a functional surface of  $\alpha$ -catenin, we created an in vitro tool that is one step closer to the in cellulo machinery. Traditional methods like optical and magnetic tweezers and atomic force microscopes allow the study of single protein molecule interactions, one at a time, but are not well adapted to protein complexes and multi-protein force transductions. Our  $\mu$ FSA-based method gives collective force read-outs allowing one to analyze the mechanics of inclusive systems made by assembling multiple molecules simultaneously. In the future, this approach will allow to probe the kinetic, stoichiometry and force-dependence properties of the minimal cadherin-associated mechanosensor. Indeed, the current minimal system can be extended by adding vinculin and other catenins to analyze for example  $\alpha$ -catenin-vinculin interactions upon myosin II motor activity on actin bundles and to quantify actin bundle reinforcement as a result of this interaction. Such a system could also be expanded to other multi-protein complexes which involve relay of mechanical forces.

## METHODS AND MATERIALS

### $\mu$ FSA preparation

Process of PDMS polymerization was adapted from the method described by Xia et al. (Xia and Whitesides, 1998). PDMS curing agent and elastomer were mixed with each other in 1:10 ratio, degassed and poured on the silicon wafer. The wafer with a layer of uncured PDMS was spin-coated for consistency in PDMS thickness. PDMS was degassed again and cured at 80°C for 2 h. Curing time was strictly followed to reproduce the Young's modulus of 2 MPa. Cured PDMS was carefully peeled from the wafer before use. In these experiments, we used doublets of micropillars (3  $\mu$ m diameter, 12  $\mu$ m length and 20  $\mu$ m spacing) which were 100  $\mu$ m apart from each other.

### Protein purification and labelling

Skeletal muscle actin was purified from rabbit muscle acetone powder following the protocol adapted from the original protocol (Spudich & Watt, 1971), described in

detail in (Wioland et al., 2017). Actin was stored on ice, in 5 mM Tris pH 7.8, 200  $\mu$ M CaCl<sub>2</sub>, 200  $\mu$ M ATP, 1 mM DTT, 0.1% NaN<sub>3</sub>, for a maximum duration of 4 weeks. Actin was labelled on accessible surface lysines of F-actin, with Alexa-488 succinimidyl ester (Life Technologies). The detailed protocol to label actin is published in (Ciobanasu et al., 2015). In the  $\mu$ FSA assay, the actin labelling fraction was 12%. Myosin II was purified from fresh rabbit skeletal muscle as previously published (Pollard, 1982). Briefly, muscle grinding in 0.5 M KCl, 0.1 M K<sub>2</sub>HPO<sub>4</sub> allows Myosin II extraction. Actin filaments are removed by centrifugation. Myosin II was then submitted to cycles of precipitation by dilution in low salt buffers, centrifugation and resuspension in high salt buffers. Myosin was finally dialyzed in 20 mM KH<sub>2</sub>PO<sub>4</sub>/K<sub>2</sub>HPO<sub>4</sub> pH 7.5, 0.5 M KCl, 1 mM EDTA. The addition of 50% glycerol ensures long term storage at -20°C.

Full-length 6x his-tagged mouse  $\alpha$ -catenin cloned in the pDW363 was expressed in *E. Coli* BL21 (Invitrogen). After transformation, bacteria were grown in 4 L of LB medium containing 0.1 mg/ml of ampicillin at 37°C until absorbance reached 0.8 at 600 nm. The induction was performed by adding 1 mM isopropyl  $\beta$ -d-1-thiogalactopyranoside and incubating at 16°C for 16 h. After centrifugation, the pellet was lysed by 50 mM Tris, pH 7.8, 500 mM NaCl, 1 mM  $\beta$ -mercaptoethanol (BME), 10  $\mu$ g/ml benzamidine and 1 mM PMSF. The lysate was loaded on Ni-NTA (Ni<sup>2+</sup>-nitrilotriacetic acid)-Agarose (Macherey-Nalgene), washed with 50 mM Tris pH 7.8, 500 mM NaCl, 20 mM Imidazole and 1 mM BME and eluted with 50 mM Tris pH 7.8, 500 mM NaCl, 100 mM Imidazole and 1 mM BME.  $\alpha$ -catenin was applied to a gel filtration column (Superdex 200, 16/60, GE Healthcare) for further purification, eluted in 20 mM Tris, pH 7.8, 150 mM KCl, 1 mM BME, frozen in liquid nitrogen, and stored at -80°C.

## $\mu$ FSA patterning

Micropillar arrays were first activated with UV light for 15 min (UVO Cleaner, Jelight Company) and incubated with 0.1% w/v poly-L-lysine (PLL) for 30 min. They were then passivated for 1 h with 100 mg/ml poly(ethylene glycol) succinimidyl valerate (PEG-SVA) freshly dissolved in 10 mM HEPES (pH 8.6) and rinsed with PBS.  $\mu$ FSAs were then patterned using a Digital Mirror Device (Primo, Alveole) mounted on an inverted Olympus IX83 inverted microscope), allowing illumination with ultraviolet light (375 nm) passing through a digital photomask. Each time before patterning, a new image of micropillars was taken and used as a mask while patterning. This gave the perfect alignment of the mask with the micropillars. Patterning was done with energy dosage of 1500 mJ/mm in the presence of photo initiator (Alveole).  $\mu$ FSAs were then rinsed with 1X PBS to remove traces of photo ini-

tiator, then again with 1X protein coating buffer (50 mM Tris pH 7.5, 150 mM NaCl, 0.1 mM EDTA and 0.25 mM DTT) to make micropillar environment conducive for  $\alpha$ -catenin attachment.  $\mu$ FSAs were, then, incubated with 1 mg/ml purified recombinant  $\alpha$ -catenin for 10 min at room temperature, then washed and blocked with 1% BSA for 20 min and thoroughly rinsed with protein. Protein coated micropillars were then placed in an imaging chamber (Interchangeable coverslip dish, Bioptech) and submerged in freshly prepared actin polymerization mix containing myosin II, unlabeled G-actin and 2% fluorescently labelled G-actin. All the steps were performed carefully to avoid any drying of the micropillars. For the condition with no  $\alpha$ -catenin coating, micropillars were directly blocked with 1% BSA after patterning. As a control, no myosin II experiments were also performed.

## Actin polymerization mix

The actin polymerization protocol was adapted from Ciobanasu et al. (Ciobanasu et al., 2015). Fluorescence buffer (2X) was prepared by mixing 20 mM Tris pH 7.8, 0.4 mM CaCl<sub>2</sub>, 0.8% methylcellulose, 10 mM DABCO, 40 mM DTT and 2% BSA. KME (20X) contained 500 mM KCl, 40 mM MgCl<sub>2</sub> and 4 mM EGTA. ATP regenerating mix (20X) was made with 40 mM ATP, 40 mM MgCl<sub>2</sub>, 200 mM creatine phosphate and 70 U/ml creatine phosphokinase. Final actin mix, that was prepared on ice and added to the micropillars, contained: 1X Fluorescence buffer, 1X KME, 1X ATP regeneration mix, 1% BSA and various concentration of actin and myosin II as indicated in the main text. G-actin buffer for actin dilution contained 2 mM Tris pH 7.8, 0.2 mM ATP, 0.5 mM DTT, 0.1 mM CaCl<sub>2</sub> and 1 mM NaN<sub>3</sub>. Myosin II dilution buffer was made of 20 mM Tris (pH 7.8), 250 mM KCl and 1 mM DTT.  $\alpha$ -catenin buffer was composed of 50 mM Tris pH 7.5, 150 mM NaCl, 0.1 mM EDTA and 0.25 mM DTT. All the chemicals were bought from Sigma-Aldrich.

## Imaging

Images were taken with a 20X objective on an Olympus IX81 inverted microscope equipped with a Andor camera at the rate of 1 frame/s. To capture the deflection of the micropillars, the actin filaments labelled with Alexa-488 and micropillars (in bright field) were imaged sequentially.

## Image analysis and force measurement

Images were analyzed using ImageJ and MATLAB. TrackMate plugin in ImageJ was used to ascertain the coordinates of micropillar center and calculate sub-pixel



deflections. Image of the micropillars taken prior to actin filament attachment was considered as the resting position for the micropillars and was used for deflection calculation.

Force was calculated by the linear theory of elasticity,

$$F = k \cdot x = \left( \frac{3}{4} \pi E \frac{r^4}{L^3} \right) x \quad (1)$$

where E is the Young's modulus, k is the spring constant and r, L & x are the radius, length and deflection of the micropillar (du Roure et al., 2005; Gupta et al., 2015; Tan et al., 2003). The rate of force increase was extracted by fitting a slope to the initial phase of the force overtime curves (Figure S2).

## Statistics

For experimental data, statistical analysis was done by two-tailed student *t*-test. Data were obtained from three independent experiments.

## ACKNOWLEDGMENTS

This work was supported by the European Research Council (Grant No. CoG-617233). This work was also supported by ARC Foundation (Grant N° PJA 20151203185 as well as LABEX Who Am I? (ANR-11-LABX-0071), the Ligue Contre le Cancer (Equipe labellisée 2019), and the Agence Nationale de la Recherche (POLCAM, ANR-17-CE13-0013). We thank Hong Wang for the production of purified  $\alpha$ -catenin. The authors acknowledge the ImagoSeine core facility of the IJM and France-Biolmaging (ANR-10-INBS-04) infrastructures. The authors thank Laurent Blanchoin and Manuel Théry for valuable advice and sharing material in the early stages of this study. The authors also thank the members of cell adhesion and mechanics team at Institut Jacques Monod and Laboratoire d'Enzymologie et Biochimie Structurales team at Centre National de la Recherche Scientifique (CNRS), Gif-sur-Yvette.

## CONFLICT OF INTEREST


The authors declare no conflict of interest.

## AUTHOR CONTRIBUTIONS

René Marc Mège and Benoit Ladoux designed the research. Surabhi Sonam performed experiments; Surabhi Sonam, René Marc Mège and Christophe Le Clainche analyzed the data. Antoine Jégou and Guillaume Romet-Lemonne provided G-actin and participated in discussions. Clémence Vigouroux helped with the set-up of the experimental model. Surabhi Sonam and René Marc Mège wrote the paper. Christophe Le Clainche, René Marc Mège and Benoit Ladoux oversaw


the project. All authors read the manuscript and commented on it.


## ORCID

Antoine Jégou  <https://orcid.org/0000-0003-0356-3127>

Guillaume Romet-Lemonne  <https://orcid.org/0000-0002-4938-1065>

Christophe Le Clainche  <https://orcid.org/0000-0001-5659-677X>

Benoit Ladoux  <https://orcid.org/0000-0003-2086-1556>

René Marc Mège  <https://orcid.org/0000-0001-8128-5543>

## REFERENCES

- Blanchoin, L., Boujemaa-Paterski, R., Sykes, C. & Plastino, J. (2014) Actin dynamics, architecture, and mechanics in cell motility. *Physiological Reviews*, 94, 235–263.
- Buckley, C.D., Tan, J., Anderson, K.L., Hanein, D., Volkmann, N., Weis, W.I., Nelson, W.J. & Dunn, A.R. (2014) Cell adhesion. The minimal cadherin-catenin complex binds to actin filaments under force. *Science*, 346, 1254211.
- Ciobanaru, C., Faivre, B. & Le Clainche, C. (2014) Actomyosin-dependent formation of the mechanosensitive talin-vinculin complex reinforces actin anchoring. *Nature communications*, 5, 3095.
- Ciobanaru, C., Faivre, B. & Le Clainche, C. (2015) Reconstituting actomyosin-dependent mechanosensitive protein complexes in vitro. *Nature Protocols*, 10, 75–89.
- del Rio, A., Perez-Jimenez, R., Liu, R., Roca-Cusachs, P., Fernandez, J.M. & Sheetz, M.P. (2009) Stretching single talin rod molecules activates vinculin binding. *Science*, 323, 638–641.
- Desai, R.A., Gao, L., Raghavan, S., Liu, W.F. & Chen, C.S. (2009) Cell polarity triggered by cell-cell adhesion via E-cadherin. *Journal of Cell Science*, 122:905–911.
- Discher, D.E., Janmey, P. & Wang, Y.L. (2005) Tissue cells feel and respond to the stiffness of their substrate. *Science*, 310, 1139–1143.
- du Roure, O., Saez, A., Buguin, A., Austin, R.H., Chavrier, P., Silberzan, P. & Ladoux, B. (2005) Force mapping in epithelial cell migration. *PNAS*, 102, 2390–2395.
- Finer, J.T., Simmons, R.M. & Spudis, J.A. (1994) Single myosin molecule mechanics: piconewton forces and nanometre steps. *Nature*, 368, 113–119.
- Ganz, A., Lambert, M., Saez, A., Silberzan, P., Buguin, A., Mege, R.M. & Ladoux, B. (2006) Traction forces exerted through N-cadherin contacts. *Biologie Cellulaire*, 98, 721–730.
- Grashoff, C., Hoffman, B.D., Brenner, M.D., Zhou, R., Parsons, M., Yang, M.T., McLean, M.A., Sligar, S.G., Chen, C.S., Ha, T. & Schwartz, M.A. (2010) Measuring mechanical tension across vinculin reveals regulation of focal adhesion dynamics. *Nature*, 466, 263–266.
- Gupta, M., Kocgozlu, L., Sarangi, B.R., Margadant, F., Ashraf, M. & Ladoux, B. (2015) Micropillar substrates: a tool for studying cell mechanobiology. *Methods in Cell Biology*, 125, 289–308.
- Kim, T.J., Zheng, S., Sun, J., Muhamed, I., Wu, J., Lei, L., Kong, X., Leckband, D.E. & Wang, Y. (2015) Dynamic visualization of alpha-catenin reveals rapid, reversible conformation switching between tension states. *Current Biology*, 25, 218–224.
- Ladoux, B., Anon, E., Lambert, M., Rabodzey, A., Hersen, P., Buguin, A., Silberzan, P. & Mege, R.M. (2010) Strength dependence of cadherin-mediated adhesions. *Biophysical Journal*, 98, 534–542.
- le Duc, Q., Shi, Q., Blonk, I., Sonnenberg, A., Wang, N., Leckband, D. & de Rooij, J. (2010) Vinculin potentiates E-cadherin mechanosensing and is recruited to actin-anchored sites within adherens junctions in

- a myosin II-dependent manner. *The Journal of cell biology*, 189, 1107–1115.
- Maier, T. & Haraszti, T. (2015) Reversibility and viscoelastic properties of micropillar supported and oriented magnesium bundled F-actin. *Plos One*, 10, e0136432.
- Mege, R.M. & Ishiyama, N. (2017) Integration of cadherin adhesion and cytoskeleton at adherens junctions. *Cold Spring Harbor perspectives in biology*, 9, a028738.
- Melero, C., Kolmogorova, A., Atherton, P., Derby, B., Reid, A., Jansen, K. & Ballestrem, C. (2019) Light-induced molecular adsorption of proteins using the PRIMO system for micro-patterning to study cell responses to extracellular matrix proteins. *Journal of visualized experiments: JoVE*, 159, 60092
- Pasturel, A., Strale, P.O. & Studer, V. (2019) A generic widefield topographical and chemical photopatterning method for hydrogels. *BioRxiv*, <https://doi.org/10.1101/370882>.
- Pollard, T.D. (1982) Myosin purification and characterization. *Methods in Cell Biology*, 24, 333–371.
- Reymann, A.C., Boujemaa-Paterski, R., Martiel, J.L., Guerin, C., Cao, W., Chin, H.F., De La Cruz, E.M., Thery, M. & Blanchoin, L. (2012) Actin network architecture can determine myosin motor activity. *Science*, 336, 1310–1314.
- Roos, W., Ulmer, J., Grater, S., Surrey, T. & Spatz, J.P. (2005) Microtubule gliding and cross-linked microtubule networks on micropillar interfaces. *Nano Letters*, 5, 2630–2634.
- Roos, W.H., Roth, A., Konle, J., Presting, H., Sackmann, E. & Spatz, J.P. (2003) Freely suspended actin cortex models on arrays of microfabricated pillars. *Chemphyschem*, 4, 872–877.
- Saez, A., Anon, E., Ghibauda, M., du Roure, O., Di Meglio, J.M., Hersen, P., Silberzan, P., Buguin, A. & Ladoux, B. (2010) Traction forces exerted by epithelial cell sheets. *Journal of Physics: Condensed Matter*, 22, 194119.
- Sarangi, B.R., Gupta, M., Doss, B.L., Tissot, N., Lam, F., Mege, R.M., Borghi, N. & Ladoux, B. (2017) Coordination between intra- and extracellular forces regulates focal adhesion dynamics. *Nano Letters*, 17, 399–406.
- Seddiki, R., Narayana, G., Strale, P.O., Balcioglu, H.E., Peyret, G., Yao, M., Le, A.P., Teck, L.C., Yan, J., Ladoux, B. & Mege, R.M. (2017) Force-dependent binding of vinculin to alpha-catenin regulates cell-cell contacts stability and collective cell behavior. *Molecular Biology of the Cell*, 29, 380–388.
- Spudich, J.A. & Watt, S. (1971) The regulation of rabbit skeletal muscle contraction. I. Biochemical studies of the interaction of the tropomyosin-troponin complex with actin and the proteolytic fragments of myosin. *Journal of Biological Chemistry*, 246, 4866–4871.
- Streichfuss, M., Erbs, F., Uhrig, K., Kurre, R., Clemen, A.E., Bohm, C.H., Haraszti, T. & Spatz, J.P. (2011) Measuring forces between two single actin filaments during bundle formation. *Nano Letters*, 11, 3676–3680.
- Tan, J.L., Tien, J., Pirone, D.M., Gray, D.S., Bhadriraju, K. & Chen, C.S. (2003) Cells lying on a bed of microneedles: an approach to isolate mechanical force. *PNAS*, 100, 1484–1489.
- Thomas, W.A., Boscher, C., Chu, Y.S., Cuvelier, D., Martinez-Rico, C., Seddiki, R., Heysch, J., Ladoux, B., Thiery, J.P., Mege, R.M. & Dufour, S. (2013) Alpha-Catenin and vinculin cooperate to promote high E-cadherin-based adhesion strength. *Journal of Biological Chemistry*, 288, 4957–4969.
- Trichet, L., Digabel, J.L., Hawkins, R.J., Vedula, S.R., Gupta, M., Ribault, C., Hersen, P., Voituriez, R. & Ladoux, B. (2012) Evidence of a large-scale mechanosensing mechanism for cellular adaptation to substrate stiffness. *PNAS*, 109, 6933–6938.
- Vedula, S. R., Leong, M. C., Lai, T. L., Hersen, P., Kabla, A. J., Lim, C. T. & Ladoux, B. (2012) Emerging modes of collective cell migration induced by geometrical constraints. *PNAS*, 109, 12974–12979.
- Vicente-Manzanares, M., Ma, X., Adelstein, R. S., & Horwitz, A.R. (2009) Non-muscle myosin II takes centre stage in cell adhesion and migration. *Nature Reviews Molecular Cell Biology*, 10, 778–790.
- Wioland, H., Guichard, B., Senju, Y., Myram, S., Lappalainen, P., Jegou, A., & Romet-Lemonne, G. (2017) ADF/cofilin accelerates actin dynamics by severing filaments and promoting their depolymerization at both ends. *Current Biology*, 27, 1956–1967.e1957.
- Wolfenson, H., Yang, B., & Sheetz, M.P. (2019) Steps in mechanotransduction pathways that control cell morphology. *Annual Review of Physiology*, 81, 585–605.
- Xia, Y., & Whitesides, G.M. (1998) Soft lithography. *Angewandte Chemie (International Ed. in English)*, 37, 550–575.
- Yao, M., Qiu, W., Liu, R., Efremov, A.K., Cong, P., Seddiki, R., Payre, M., Lim, C.T., Ladoux, B., Mege, R.M. & Yan, J. (2014) Force-dependent conformational switch of alpha-catenin controls vinculin binding. *Nature communications*, 5, 4525.
- Yonemura, S., Wada, Y., Watanabe, T., Nagafuchi, A. & Shibata, M. (2010) alpha-Catenin as a tension transducer that induces adherens junction development. *Nature Cell Biology*, 12, 533–542.

**How to cite this article:** Sonam, S., Vigouroux, C., Jégou, A., Romet-Lemonne, G., Le Clainche, C., Ladoux, B., & Mège, R. M. (2021). Direct measurement of near-nano-Newton forces developed by self-organizing actomyosin fibers bound  $\alpha$ -catenin. *Biology of the Cell*, 1–9. <https://doi.org/10.1111/boc.202100014>